

Modeling Of Doubly Fed Induction Generator Based Wind Turbine With Blade Pitch Angle Control

Ilakranti Gupta *, Supriya Tripathi**

* PG Scholar (M.Tech 4TH Semester), Electrical Department, Bhilai Institute Of Technology Durg, India.

**Associate Professor, Electrical Department, Bhilai Institute Of Technology Durg, India,

stripathi@bitdurg.ac.in

Email id:ilakranti10@gmail.com

Abstract

Many large wind farms are employing doubly fed induction generator (DFIG) variable speed wind turbines. With the rising penetration of wind power into electricity networks, increasingly comprehensive studies are required to identify the interaction between the wind farm and the power system. These require accurate models of doubly fed induction generator wind turbines and their associated control and protection circuits. The Pitch angle control is the most common means for adjusting the aerodynamic torque of the wind turbine when wind speed is above rated speed and various controlling variables may be chosen, such as wind speed, generator speed and generator power. As conventional pitch control usually use PI controller, the mathematical model of the system should be known well. The block diagram of the proposed speed control system which consists of speed controller, actuator model and the turbine linearized model is simulated by Matlab-Simulink software package. The simulation results show that the controller accurately adjusts the blade pitch angle to set the wind turbine power output to its reference value.

Keywords: doubly fed induction generator, variable speed drive, wind turbine power generation power coefficient, tip speed ratio, blade pitch angle.

1. Introduction

India has one of the fifth largest wind power installed capacity in the world. The DFIG is a currently a choice for multi MW wind turbine. The aim of wind turbine is continuously increase output power and to achieve optimum aerodynamic efficiency. It is a viable alternative to adjust speed over a wide range at minimal cost. It can be used for variable frequency variable speed technology in wind energy conversion system and with increased penetration of wind power into electrical grids, DFIG wind turbines are largely deployed due to their variable speed feature and hence influencing system dynamics. This has created an interest in developing suitable models for DFIG to be integrated into power system studies. The continuous trend of having high penetration of wind power, in recent years, has made it necessary to introduce new practices. The schematic diagram of DFIG is shown in figure 1.

This paper describes the modeling of the various components in a pitch controlled wind energy system. It also describes the design of the pitch controller and discusses the response of the pitch-controlled system to wind velocity variations. The pitch control system is found to have a large output power variation and a large settling time.

The pitch function gives full control over the mechanical power and if the most common method is used for the variable speed wind turbines. At wind speeds below the rated power of the generator, the pitch angle is at its maximum though it can be lower to help the turbine accelerate faster. Above the rated wind speed, the pitch angle is controlled to keep the generator power at rated power by reducing the angle of blades.

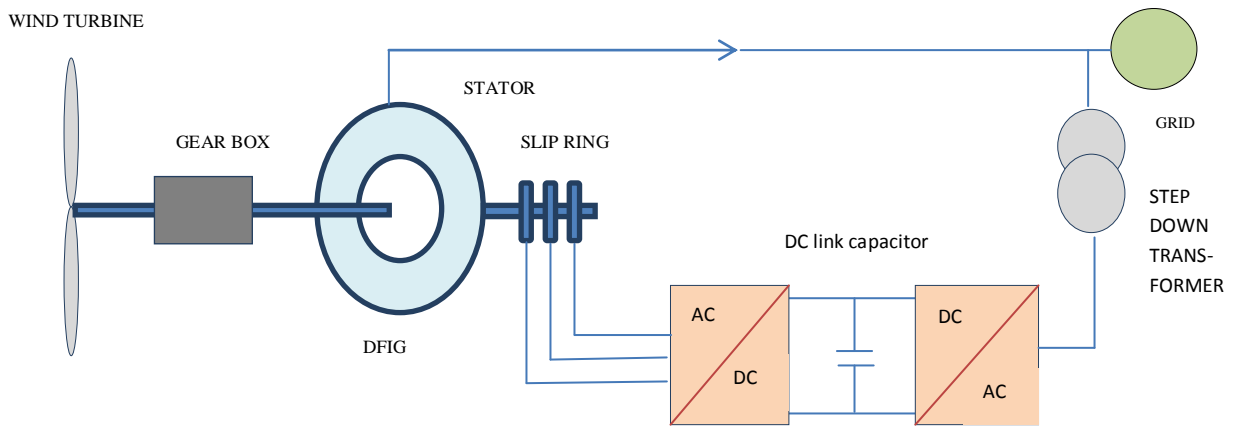


Figure: 1 Schematic diagram of doubly fed induction generator

The pitch control system is one of the most widely used control techniques to regulate the output power of a wind turbine generator. The method relies on the variation in the power captured by the turbine as the pitch angle of the blades is changed. Hydraulic actuators are used to vary the pitch angle. The wind turbine generator describes the design of the pitch controller and discusses the performance of the system in the presence of disturbances.

The control system consists of two controllers are inverter controller that keeps the load voltage constant and the pitch controller acting on the blades angle by using simulation.

II. Dynamic Modeling Of Wind Turbine

1. Wind Turbine Model

In steady-state at fixed turbine speed for a lossless DFIG system, the mechanical power from the wind turbine applied to the shaft is $P_m = P_s + P_r$. It follows that:

$$P_r = P_m - P_s = T_m \omega_r - T_{em} \omega_s = -T_m \left(\frac{\omega_s - \omega_r}{\omega_s} \right) \omega_s = -s T_m \omega_s = -s P_s \quad (1)$$

Where s is defined as the slip of the generator:

$$s = \frac{\omega_s - \omega_r}{\omega_s} \quad (2)$$

Therefore if the maximum slip is limited, say to 0.3, the rotor winding converters can be rated as a fraction of the induction generator rated power. This is typically around $\pm 30\%$ for DFIG in wind power generation systems gives a slip range of ± 0.3 . This is one key advantage of the DFIG system over fully-rated power electronic systems.

From the above relationships, the stator and rotor power are $P_s = P_m/(1-s)$ and $P_r = -s P_m/(1-s)$, respectively. To consider the mechanical power change during different rotor speeds, the following analysis is carried out with all terms in per unit values. The slip is assumed to vary from a sub-synchronous value of +0.35 to a super-synchronous value of -0.35.

The per unit output power from wind turbine is:

$$P_m = C_{p_pu} V_{wind_pu}^3 \quad (3)$$

Here we use the example wind turbine model in MATLAB (The Mathworks Inc., 2008):

$$C_p(\lambda, \beta) = c_1 \left(\frac{c_2}{\lambda_i} - c_3 \beta - c_4 \right) e^{-\frac{c_5}{\lambda_i}} + c_6 \lambda, \quad (4)$$

$$\frac{1}{\lambda_i} = \frac{1}{\lambda + 0.08\beta} - \frac{0.035}{\beta^3 + 1}, \quad (5)$$

with the coefficients as $c_1 = 0.5176$, $c_2 = 116$, $c_3 = 0.4$, $c_4 = 5$, $c_5 = 21$ and $c_6 = 0.0068$.

$$\lambda = \frac{\omega_r R}{V_{wind}} \quad (6)$$

is the tip-speed ratio.

The maximum value of C_p is 0.48 when $\beta = 0$ for $\lambda = 8.1$. These are defined as base values for per unit calculations. Here base wind speed is 12 m/s, gear ratio is 10, rotor radius is 5.16m. When $s = -0.2$, C_p is 0.48 then P_m is 1.0 pu ideally. Hence for 2 pole-pair generator,

$$s = \frac{\omega_s - \omega_r}{\omega_s}, \quad \omega_{r_pu} = 1 - s, \quad \lambda = \frac{\omega_r R}{V_{wind}} = (1 - s) \frac{5\pi \times 5.16}{12} = 6.751(1 - s) = c_7(1 - s)$$

Then at the base wind speed, the expression of P_m in terms of slip s is

$$P_m = \frac{C_p}{0.48} = \frac{1}{0.48} \left[c_1 \left(\frac{c_2}{\lambda_i} - c_4 \right) e^{-\frac{c_5}{\lambda_i}} + c_6 c_7 (1 - s) \right], \quad \frac{1}{\lambda_i} = \frac{1}{c_7(1 - s)} - 0.035 \quad (7)$$

The above analysis is carried out in MATLAB programming, with the power flow result shown in Figure. 2 shows how the rotor and stator power vary as the rotor slip changes from sub- to super-synchronous modes. The speed of the rotor has to change as wind speed changes in order to track the maximum power point of the aerodynamic system. Slip, s , therefore is related to incident wind speed. In this case, a slip of -0.2 occurs with rated wind speed (12 ms^{-1}). As wind speed drops, slip has to increase and in this case has a maximum value of 0.35.

It is clear that the mechanical power, P_m , reaches its peak at super-synchronous speed when $s = -0.2$. When rotating at the synchronous speed ($s = 0$), the DFIG supplies all the power via the stator winding, with no active power flow in the rotor windings and their associated converters. Note that at $s=0$, the stator power is maximum. As the wind speed increases, the rotational speed must also increase to maintain optimum tip-speed ratios. In such circumstances, the machine operates at super-synchronous speeds ($s < 0$). The mechanical power flows to the grid through both the stator windings and the rotor windings and their converter. For example, at $s=-0.2$, P_s is 0.8pu and P_r is 0.2 pu giving a total generated power of 1pu. At lower wind speeds, the blades rotate at a sub-synchronous speed ($s > 0$). In such circumstances, the rotor converter system will absorb power from the grid connection to provide excitation for rotor winding. For example, at $s=0.2$, P_s is 0.8pu but P_r is -0.2 pu giving a total generated power of 0.6pu. With such a control scheme it is possible to control the power extracted from the aerodynamic system such that the blade operates at the optimum aerodynamic efficiency (thereby extracting as much energy as is possible) by adjusting the speed of rotation according to the incident wind speed.

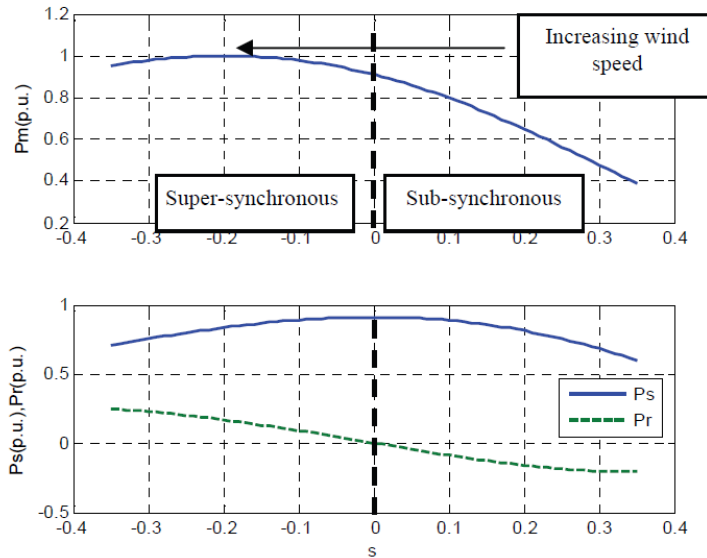


Figure: 2 Doubly-fed induction generation system power flows.

2. DFIG Model

To describe the control scheme, the general Park’s model of an induction machine is introduced. Using the motor convention in a static stator-oriented reference frame, without saturation, the voltage vector equations are:

$$\vec{v}_s = R_s \vec{i}_s + \frac{d\vec{\psi}_s}{dt} \tag{8}$$

$$\vec{v}_r = R_r \vec{i}_r + \frac{d\vec{\psi}_r}{dt} - j\omega \vec{\psi}_r \tag{9}$$

Where \vec{v}_s is the stator voltage imposed by the grid. The rotor voltage is controlled by the rotor-side converter and used to perform generator control.

The flux vector equations are:

$$\vec{\psi}_s = L_s \vec{i}_s + L_m \vec{i}_r \tag{10}$$

$$\vec{\psi}_r = L_m \vec{i}_s + L_r \vec{i}_r \tag{11}$$

where L_s and L_r are the stator and rotor self-inductances: $L_s = L_m + L_{ls}$, $L_r = L_m + L_{lr}$.

Under stator-flux orientation (SFO), in dq -axis component form, the stator flux equations are:

$$\begin{cases} \psi_{sd} = L_s i_{sd} + L_m i_{rd} = \psi_s = L_m i_{ms} \\ \psi_{sq} = 0 \end{cases} \tag{12}$$

$$\tag{13}$$

Defining leakage factor

$$\sigma = 1 - \frac{L_m^2}{L_s L_r} \tag{14}$$

and equivalent inductance as

$$L_o = \frac{L_m^2}{L_s} \tag{15}$$

The rotor voltage and flux equations are (scaled to be numerically equal to the ac per-phase values):

$$\begin{cases} v_{rd} = R_r i_{rd} + \sigma L_r \frac{di_{rd}}{dt} - \omega_{slip} \sigma L_r i_{rq} \end{cases} \quad (16)$$

$$\begin{cases} v_{rq} = R_r i_{rq} + \sigma L_r \frac{di_{rq}}{dt} + \omega_{slip} (L_o i_{ms} + \sigma L_r i_{rd}) \end{cases} \quad (17)$$

$$\begin{cases} \psi_{rd} = \frac{L_m^2}{L_s} i_{ms} + \sigma L_r i_{rd} \end{cases} \quad (18)$$

$$\begin{cases} \psi_{rq} = \sigma L_r i_{rq} \end{cases} \quad (19)$$

where the slip angular speed is $\omega_{slip} = \omega_s - \omega_r$.

The stator flux angle is calculated from

$$\begin{cases} \psi_{s\alpha} = \int (v_{s\alpha} - R_s i_{s\alpha}) dt \\ \psi_{s\beta} = \int (v_{s\beta} - R_s i_{s\beta}) dt \end{cases}, \theta_s = \tan^{-1} \left(\frac{\psi_{s\beta}}{\psi_{s\alpha}} \right) \quad (20)$$

where θ_s is the stator-flux vector position.

Rotor excitation current control is realised by controlling rotor voltage. The i_{rd} and i_{rq} error signals are processed by associated PI controllers to give v_{rd} and v_{rq} , respectively. From the rotor voltage equations (16),(17) define

$$\begin{cases} v'_{rd} = R_r i_{rd} + \sigma L_r \frac{di_{rd}}{dt} \\ v'_{rq} = R_r i_{rq} + \sigma L_r \frac{di_{rq}}{dt} \end{cases} \quad (21)$$

To ensure good tracking of the rotor dq -axis currents, compensation terms are added to v'_{rd} and v'_{rq} to obtain the reference voltages v_{rd}^* and v_{rq}^* according to

$$\begin{cases} v_{rd}^* = v'_{rd} - \omega_{slip} \sigma L_r i_{rq} \end{cases} \quad (23)$$

$$\begin{cases} v_{rq}^* = v'_{rq} + \omega_{slip} (L_o i_{ms} + \sigma L_r i_{rd}) \end{cases} \quad (24)$$

The electromagnetic torque is

$$T_e = -\frac{3}{2} p \text{Im} \{ \bar{\psi}_s \bar{i}_r^* \} = -\frac{3}{2} p L_o i_{ms} i_{rq} \quad (25)$$

For the stator-voltage oriented control the above equation is an approximation. However, for stator-flux orientation, the stator flux current i_{ms} is almost fixed to the stator voltage. For torque mode control, since it is difficult to measure the torque, it is often realised in an open-loop manner. The torque can be controlled by the q -axis component of the rotor current i_{rq} . Therefore, the q -axis reference current, i_{rq}^{ref} can be determined from the reference torque T_e^{ref} as

$$i_{rq}^{ref} = -\frac{2T_e^{ref}}{3pL_o i_{ms}} = -\frac{2T_e^{ref}}{3p\psi_s} \quad (26)$$

The voltage equations in synchronously rotating dq -axis reference frame are:

$$\begin{cases} v_{cd} = Ri_{cd} + L_{choke} \frac{di_{cd}}{dt} - \omega_e L_{choke} i_{cq} + v_{cd1} \\ v_{cq} = Ri_{cq} + L_{choke} \frac{di_{cq}}{dt} + \omega_e L_{choke} i_{cd} + v_{cq1} \end{cases} \quad (27)$$

(28)

The angular position of the grid voltage is calculated as

$$\theta_e = \int \omega_e dt = \tan^{-1} \left(\frac{v_{c\beta}}{v_{c\alpha}} \right) \quad (29)$$

where $v_{c\alpha}$ and $v_{c\beta}$ are the converter grid-side voltage stationary frame components.

The d -axis of the reference frame is aligned with the grid voltage angular position θ_e . Since the amplitude of the grid voltage is constant, v_{cq} is zero and v_{cd} is constant. The active and reactive power will be proportional to i_{cd} and i_{cq} respectively.

Assume the grid-side transformer connection is star, the converter active and reactive power flow is

$$\begin{cases} P_c = 3(v_{cd} i_{cd} + v_{cq} i_{cq}) = 3v_{cd} i_{cd} \\ Q_c = 3(v_{cd} i_{cq} + v_{cq} i_{cd}) = 3v_{cd} i_{cq} \end{cases} \quad (30)$$

(31)

which demonstrates that the real and active powers from the grid-side converter are controlled by the i_{cd} and i_{cq} components of current respectively. To realise decoupled control, similar compensations are introduced likewise in equation (30):

$$\begin{cases} v_{cd}^* = -v'_{cd} + (\omega_e L_{choke} i_{cq} + v_d) \\ v_{cq}^* = -v'_{cq} - (\omega_e L_{choke} i_{cd}) \end{cases} \quad (32)$$

(33)

The reference voltage v_{cd}^* and v_{cq}^* are then transformed by inverse-Park transformation to give 3-phase voltage v_{cab}^* for the final PWM signal generation for the converter IGBT switching.

3. Pitch Angle Control

Pitch control means that the blades can pivot upon their own longitudinal axis. The pitch control used for speed control, optimization of power production and to start and step the turbine. The pitch angle is kept constant at zero degrees until the speed reaches point D speed of the tracking characteristic. Beyond point D the pitch angle is proportional to the speed deviation from point D speed. The control system is illustrated in the following figure 3.

Pitch Control System

The turbine model uses the Wind Turbine block of the Renewables/Wind Generation library. The doubly-fed induction generator phasor model is the same as the wound rotor asynchronous machine (see the Machines library) with the following two points of difference:

1. Only the positive-sequence is taken into account, the negative-sequence has been eliminated.
2. A trip input has been added. When this input is high, the induction generator is disconnected from the grid and from C_{rotor} .

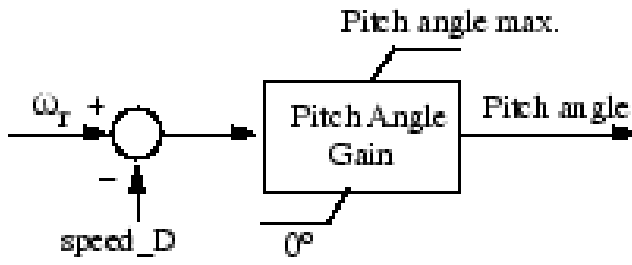


Figure:3 Turbine pitch angle model

III. Proposed Model

The pitch control method is a basic approach for controlling the rotational speed of wind turbine. The conventional blade pitch angle control strategies are developed in this part. The pitch angle reference β_{ref} , is controlled by the input values. The $C_p(\lambda, \beta)$ characteristic gives us a power coefficient, that depends on the tip speed ratio λ and the pitch angle β . The power coefficient vs tip speed ratio curve with different value of pitch angle is shown in figure 4. Because of the fluctuating nature of the wind speed the output of the wind turbine varies. At the high wind speed, fatigue damage can be occurred to the mechanical parts of the wind turbine. By controlling the pitch angle the output power can be limited as the wind turbine rotor power coefficient decreases with the increase of pitch angle. At the high wind speed the automatically activated pitch controller keep the output power within rated level by increasing the value of pitch angle.

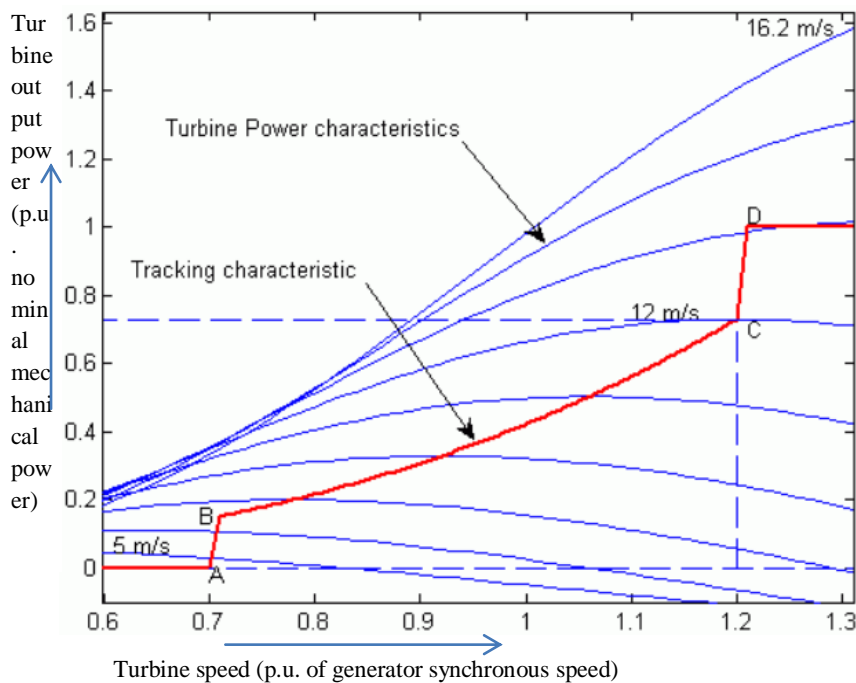


Figure:4 Turbine power characteristics (pitch angle $\beta = 0$ deg)

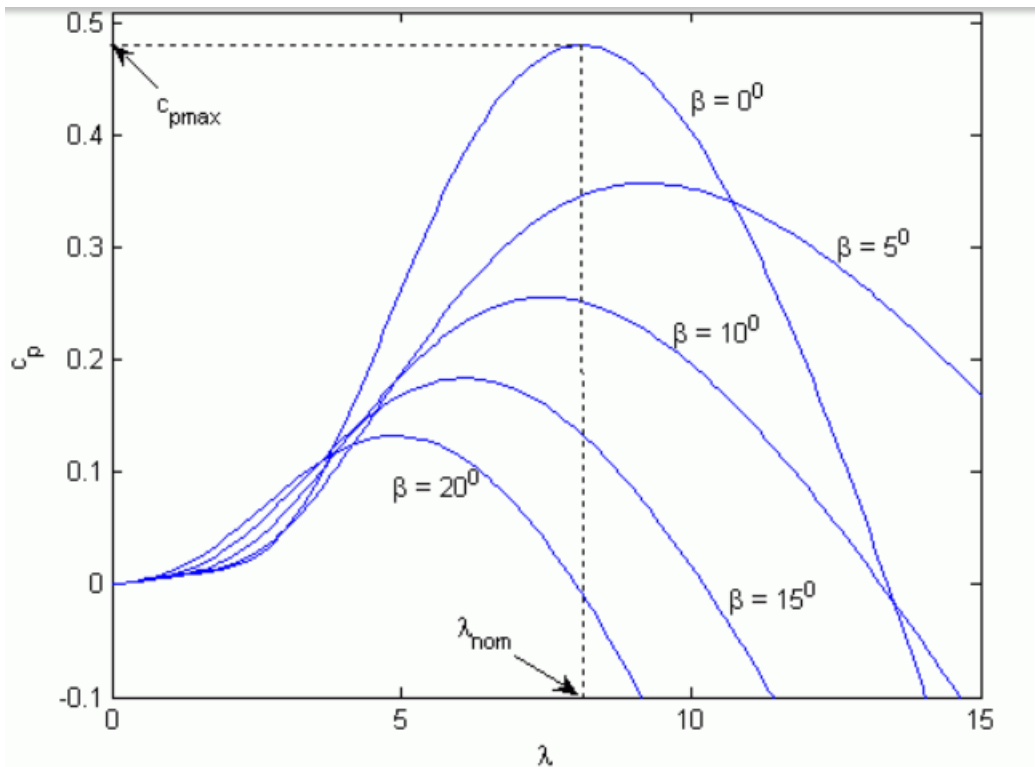


Figure:4 Power coefficient vs tip speed ratio Curve with different value of pitch Angle

IV. Expected Simulation Results

Figure:5 shows the time of starting the wind the pitch angle $\hat{\alpha}$ is set at a value of 0° to a power variation ranging from 0 to about 1.6MW (Figure. 6). Then, this angle varies vertically to reach such values so as to maintain constant power, in a time which varies depending on the speed of the selected pitch angle ($12^\circ/\text{s}$).

The setting angle comes into play and goes from 0° to 24° in near 2s [11.9s , 13.9s] the influence of this passage see this on the electrical power generated, exceeded 9% of the power beyond the set point (nominal power) Figure. 6.

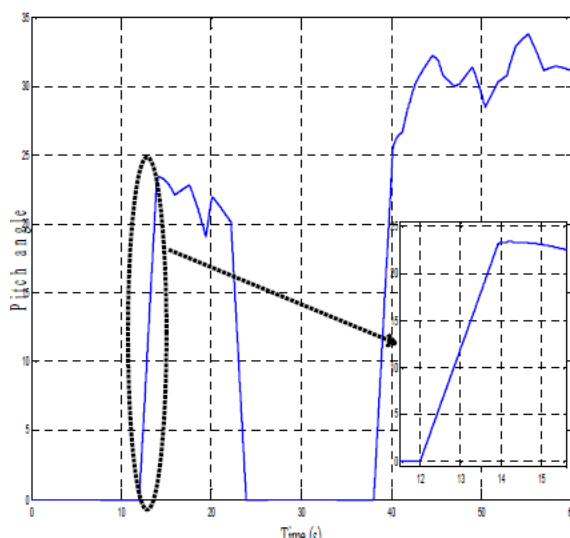


Figure:5. Pitch angle (variable speed $12^\circ/\text{s}$)

At the 24s, the pitch angle $\hat{\alpha}$, returns to 0° which implies that at that moment the wind speed dropped beyond the wind speed that produces the nominal power at 0° , therefore, the pitch system is deactivated, and resumes the regulation has the 38s .

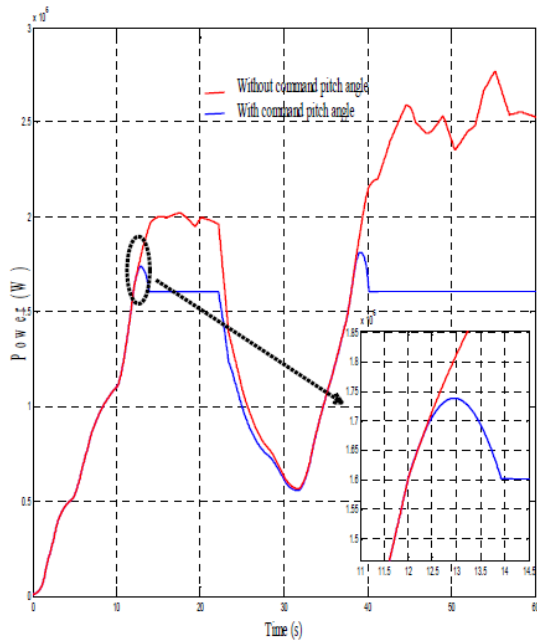


Figure: 6. Electric power generated

Figure. 7 and Figure.8 shows the simulation results for a speed variation of the pitch angle of $20^\circ/s$. At boot time the wind the pitch angle $\hat{\alpha}$ pass 0° to 24° in 1.3s near [11.9s, 13.2s] (Figure.7), a significant improvement compared to the previous configuration of $12^\circ/s$ which is 2s [11.9s, 13.9s], (Figure. 5). Rest, this configuration is used only in emergencies where the blades positioned dots feathered beings (90°) in a very short period of time.

Figure. 8 shows the effect of pitch angle $\hat{\alpha}$ of $20^\circ/s$ on the electrical power generated. At $20^\circ/s$ the effect on the power curve is remarkable, and clearly shows that the power is fully stabilized in less time and overtaking 6%. Therefore, the speed pitch angle plays a primordial role in the quality and reliability of power, but it is limited by the efforts that can withstand the pales.

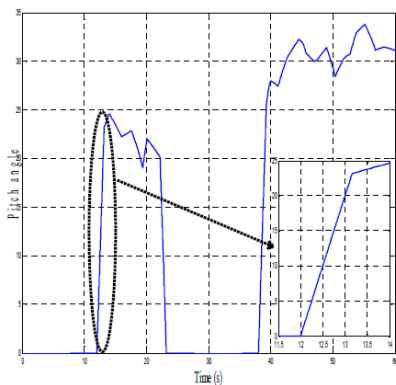


Figure:7. Pitch angle (variable speed $20^\circ/s$)

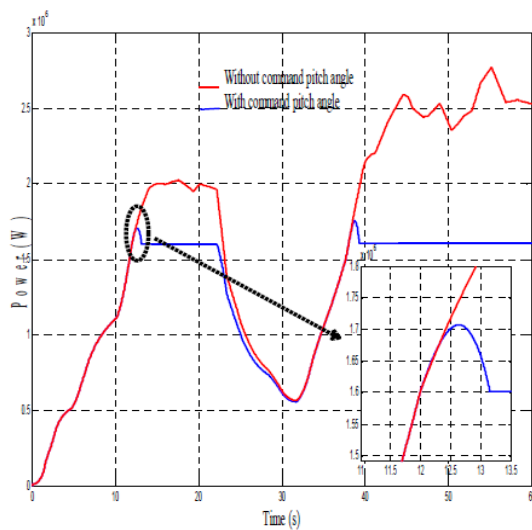


Figure:8. Electric power generated

V. Conclusions

The pitch control system is easy to implement, but the response is slow and output power variation is large. The aerodynamic power control for the variable speed wind turbine can limit the power into the turbine by reducing the angle of the blades. The pitch control characteristics were found out and the power speed characteristics were derived for various wind speeds. For a wind which gives a power greater than the nominal of the turbine, the wind turbine equipped with this system pitch allows to lower the excess power to keep it constant to ensure the continuity of the production of electrical energy provides a more level of economic performance and commercial. So the orientation of the pales, it is a protection system that reacts to the wind without cutoff action, all ensuring continuity of service.

References

- [1] By S . Muller, M. Deicke, Rikw. De Doncker, “*Doubly Fed Induction Generator Systems*”, IEEE Industry Applications Magazine May | June 2002.
- [2] Yazhou Lei, Alan Mullane, Gordon Lightbody, And Robert Yacamini , “*Modeling Of The Wind Turbine With A Doubly Fed Induction Generator For Grid Integration Studies*”, IEEE TRANSACTIONS ON ENERGY CONVERSION, VOL. 21, No. 1, March 2006
- [3] H. Abouobaida, M. Cherkaoui , “*Modeling And Control Of Doubly Fed Induction (DFIG) Wind Energy Conversion System*” , JEE
- [4] Faisal Rehman , Babar Azeem , C. A. Mehmood, S. M. Ali, B. Khan, “*Control Of Grid Interfaced Doubly Fed Induction Generator Using Adaptive SMC Improved With LVRT Enhancement*”, IEEE DOI 10.1109/Fit.2016.65, 2016
- [5] Vijay Chand Ganti, Bhim Singh, Shiv Kumar Aggarwal, And Tara Chandra Kandpal, “*DFIG-based Wind Power Conversion With Grid Power Leveling For Reduced Gusts*”, IEEE TRANSACTIONS ON SUSTAINABLE ENERGY, VOL. 3, No. 1, January 2012
- [6] J. B. Ekanayake, L. Holdsworth, X. G. Wu, And N. Jenkins, “*Dynamic Modeling Of Doubly Fed Induction Generator Wind Turbines*,” IEEE Trans. Power Syst., Vol. 18, No. 2, pp. 803–809, May 2003.
- [7] Dr. John Fletcher And Jin Yang University Of Strathclyde, Glasgow, United Kingdom Chapter 14 “*Introduction To Doubly Fed Induction Generator For Wind Power Application*” pp. 259-279.